

Competing topological and Kondo insulator phases on a honeycomb lattice

Xiao-Yong Feng,¹ Jianhui Dai,^{1,2} Chung-Hou Chung,^{3,4} and Qimiao Si⁵

¹*Condensed Matter Group, Department of Physics,
Hangzhou Normal University, Hangzhou 310036, China*

²*Department of Physics, Zhejiang University, Hangzhou 310027, China*

³*Electrophysics Department, National Chiao-Tung University, HsinChu, Taiwan, 300 R.O.C.*

⁴*National Center for Theoretical Sciences, HsinChu, Taiwan, 300 R.O.C.*

⁵*Department of Physics and Astronomy, Rice University, Houston, TX 77005, USA*

We investigate the competition between the spin-orbit interaction of itinerant electrons and their Kondo coupling with local moments densely distributed on the honeycomb lattice. We find that the model at half-filling displays a quantum phase transition between topological and Kondo insulators at a nonzero Kondo coupling. In the Kondo-screened case, tuning the electron concentration can lead to a new topological insulator phase. The results suggest that the heavy-fermion phase diagram contains a new regime with a competition among topological, Kondo-coherent and magnetic states, and that the regime may be especially relevant to Kondo lattice systems with $5d$ -conduction electrons. Finally, we discuss the implications of our results in the context of the recent experiments on SmB_6 implicating the surface states of a topological insulator, as well as the existing experiments on the phase transitions in SmB_6 under pressure and in CeNiSn under chemical pressure.

PACS numbers: 71.10.-w, 71.27.+a, 73.43.Nq, 75.70.Tj

Systems containing both itinerant electrons and local moments continue to attract intensive interests in modern condensed matter physics. The antiferromagnetic exchange coupling between the two components gives rise to the Kondo singlet ground state. Historically, the Kondo effect in a single local-moment impurity provided the understanding of the resistivity minimum in metals as well as the physics of dilute magnetic alloys and quantum nanostructures^{1,2}. In the concentrated case, consideration of the Kondo effect and its competition with magnetically ordered ground states has been playing a central role in the understanding of the novel phases and quantum criticality of heavy fermion materials³. For the half-filled limit of the Kondo lattice system, the Kondo effect gives rise to the paramagnetic Kondo insulator (KI) state^{2,4-6}.

Recently, the quantum spin Hall insulator in two dimensions (2D) and the topological insulator (TI) more generally have attracted extensive interest^{7,8}. These insulators have a charge excitation gap in the bulk, but support gapless surface states protected by time-reversal symmetry (TRS). The surface states constitute a helical liquid where the spin orientation is locked with the direction of electron momentum^{9,10}. Although they are robust against weak disorders that preserve TRS, the surface states may be influenced by magnetic impurities. For example, the conductance of 1D edge helical liquid of a 2D TI in the presence of a single magnetic impurity can exhibit a logarithmic behavior at high temperatures and goes to the unitarity limit at $T = 0$ due to the formation of a Kondo singlet^{10,11}. This is in contrast to the Kondo problem in conventional Luttinger liquids, where even very weak Coulomb interaction leads to vanishing conductance at zero temperature¹². Generally speaking, the Kondo screening of magnetic impurities on the surface of TI's may not necessarily be complete due to the

$SU(2)$ breaking of the spin-orbit coupling (SOC)¹³, and the effective RKKY interaction between the local moments can be mediated by the edge carries, leading to an in-plane noncollinear and helical order¹⁴⁻¹⁷. For magnetic impurities in TI's, previous studies have focused on the effect of *surface impurities*, i.e., magnetic impurities positioned on the surface of TI's, or coupled effectively to the surface states¹⁸. Whether and how the *bulk magnetic impurities* influence the properties of TI's is largely an open problem.

From the perspective of heavy-fermion physics, very interesting properties are emerging from materials which involve $5d$ electrons, such as the pyrochlore $\text{Pr}_2\text{Ir}_2\text{O}_7$ ¹⁹. The significant SOC of the $5d$ electrons may give rise to topologically non-trivial physics for the $5d$ electrons alone, raising the intriguing question of the interplay between topological and Kondo physics. The regime of transitions among the competing ground states represents a setting in which the effects of strong interactions on TI's may become more tractable. Furthermore, Kondo insulators themselves may become topological as a result of the symmetry properties of the hybridization matrix²⁰.

Motivated by these recent developments, in this letter we study a dense set of magnetic impurities interacting with the spin-orbit coupled itinerant electrons on the honeycomb lattice as illustrated in Fig. 1. Such a system is relevant for the graphene/magnetic moment interface and could be constructed through cold atoms in an optical lattice. The system could also be realized by growing a 2D TI on an appropriate magnetic insulating substrate; the similar heterostructures involving TI Bi_2Se_3 thin films and superconducting layers have already been fabricated by the molecular beam epitaxy technique²¹. It may very well be built based on the existing $5d$ electron based iridates on the honeycomb lattice, such as

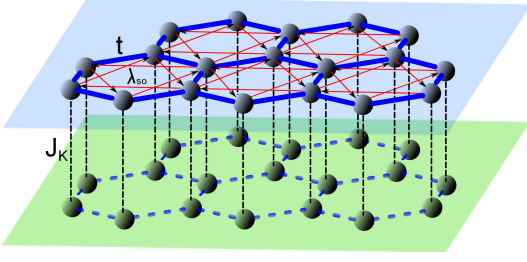


FIG. 1: Itinerant electrons moving on a honeycomb lattice while coupled vertically to the local spins on a parallel lattice.

Na_2IrO_3 ²². Finally, given that recent experiments in SmB_6 have provided tentative evidence for the surface states of a topological insulator^{23,24}, our results here on the transitions between topological insulator and Kondo coherent states lead to the intriguing question of what happens to such surface states when SmB_6 and related intermetallic systems are tuned by external or chemical pressure (see below).

The model we consider, illustrated in Fig.1, is specified by the Hamiltonian

$$H = -t \sum_{\langle ij \rangle \sigma} c_{i\sigma}^\dagger c_{j\sigma} + i\lambda_{so} \sum_{\langle\langle ij \rangle\rangle \sigma\sigma'} v_{ij} c_{i\sigma}^\dagger \sigma_{\sigma\sigma'}^z c_{j\sigma'} + J_K \sum_{\mathbf{i}} \vec{s}_{\mathbf{i}} \cdot \vec{S}_{\mathbf{i}}, \quad (1)$$

where $c_{i\sigma}$ annihilates an electron at site \mathbf{i} with spin component $\sigma = \uparrow, \downarrow$, $\vec{s}_{\mathbf{i}} = c_{i\sigma}^\dagger (\vec{\sigma}_{\sigma\sigma'}/2) c_{i\sigma'}$, and $\vec{S}_{\mathbf{i}}$ represents the local moments with $\vec{\sigma}$ being the Pauli matrices. The parameters t and λ_{so} are the nearest neighbor hopping energy and the next-nearest-neighbor *intrinsic* (Dresselhaus-type) SOC of the conduction electrons respectively, with $v_{ij} = \pm 1$ depending on the direction of hopping between the next-nearest-neighbor sites. Finally, J_K is the *antiferromagnetic* Kondo coupling between the spins of conduction electrons and local impurities. The model Eq.(1) minimally interpolates the Kane-Mele Hamiltonian ($J_K = 0$)^{9,25} and the standard Kondo lattice Hamiltonian ($\lambda_{so} = 0$). We note that recent studies have focused on the effect of Hubbard U interaction of the conduction electrons^{26–31}.

To proceed, we note that the model of Eq.(1) is connected to the Anderson lattice Hamiltonian

$$H = H_{KM} + H_{cd} + H_d, \quad (2)$$

where H_{KM} is the Kane-Mele Hamiltonian [the first two terms of Eq.(1)], $H_{cd} = V \sum_{\mathbf{i}\sigma} (c_{i\sigma}^\dagger d_{i\sigma} + h.c.)$ is the hybridization between the itinerant electrons and localized d -electrons, and $H_d = E_0 \sum_{\mathbf{i}\sigma} d_{i\sigma}^\dagger d_{i\sigma} + U \sum_{\mathbf{i}} n_{d\uparrow} n_{d\downarrow}$ is for the local electrons with E_0 being the local energy level and U the on-site Coulomb repulsion of local electrons. The models described by Eqs.(1) and (2) are equivalent provided that, in the absence of SOC, the d -electrons are in the Kondo regime (U is sufficient large and E_0 is well

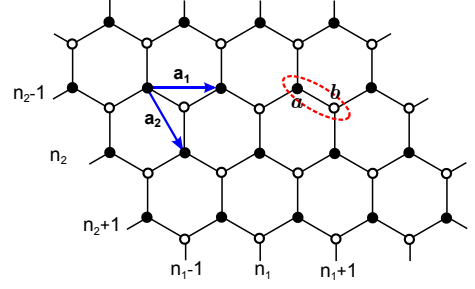


FIG. 2: The unit cell and primitive translation vectors.

below the Fermi energy (E_F) of the conduction band). In this regime, $J_K \sim V^2 [\frac{1}{E_F - E_0} + \frac{1}{U - E_F + E_0}]$. Our calculations will be carried out in Eq.(2). As our focus is on the competition between the TI and KI at half filling, we shall mainly consider the paramagnetic states.

In the momentum \mathbf{k} -space, the conduction electron part of Hamiltonian takes the form of $H_{KM} = \sum_{\mathbf{k}\sigma} C_{\mathbf{k}\sigma}^\dagger M_{\mathbf{k}\sigma} C_{\mathbf{k}\sigma}$, with $C_{\mathbf{k}\sigma}^\dagger = (c_{a,\mathbf{k}\sigma}^\dagger, c_{b,\mathbf{k}\sigma}^\dagger)$ and

$$M_{\mathbf{k}\sigma} = \begin{pmatrix} \sigma \Lambda_{\mathbf{k}} - \mu & \epsilon_{\mathbf{k}} \\ \epsilon_{\mathbf{k}}^* & -\sigma \Lambda_{\mathbf{k}} - \mu \end{pmatrix}, \quad (3)$$

where, $\sigma = +1$ and -1 refers to spin up and spin down, $\Lambda_{\mathbf{k}} = 2\lambda_{so} [\sin k_1 - \sin k_2 - \sin(k_1 - k_2)]$, $\epsilon_{\mathbf{k}} = -t(1 + e^{-ik_1} + e^{-ik_2})$. We have included the chemical potential μ -term to control the electron filling. The subscripts a and b denote two sublattices of the honeycomb lattice as shown in Fig.2. Each unit cell has two adjacent a, b sites, and the primitive vectors are \mathbf{a}_1 and \mathbf{a}_2 .

For the local electrons, we consider the large- U limit and utilize the slave-boson method¹. The local electrons are expressed as $d_{i\sigma}^\dagger = f_{i\sigma}^\dagger b_i$, with $f_{i\sigma}^\dagger$ and b_i being respectively fermionic and bosonic operators satisfying the constraint $b_i^\dagger b_i + \sum_{\sigma} f_{i\sigma}^\dagger f_{i\sigma} = 1$. Introducing the basis $\Psi_{\mathbf{k}\sigma}^\dagger = (c_{a,\mathbf{k}\sigma}^\dagger, c_{b,\mathbf{k}\sigma}^\dagger, f_{a,\mathbf{k}\sigma}^\dagger, f_{b,\mathbf{k}\sigma}^\dagger)$ in the \mathbf{k} -space, the mean-field Hamiltonian is expressed as $H_{MF} = \sum_{\mathbf{k}\sigma} \Psi_{\mathbf{k}\sigma}^\dagger H_{\mathbf{k}\sigma} \Psi_{\mathbf{k}\sigma}$ with

$$H_{\mathbf{k}\sigma} = \begin{pmatrix} M_{\mathbf{k}\sigma} & rV \cdot I \\ rV \cdot I & (E_0 + \lambda) \cdot I \end{pmatrix}. \quad (4)$$

Here, I is a 2×2 identity matrix, $r = \langle b \rangle$ is the condensation density of the bosons, and λ is the Lagrange multiplier introduced to implement the constraint. We will carry out our calculations for $N = 2$ ($\sigma = \pm 1$); a large- N generalization in the presence of SOC may also be considered³². The quasiparticle bands of the mean-field Hamiltonian Eq. (4) are degenerate for the two spin components. For each spin component, the Hamiltonian can be diagonalized (even though the matrix is 4×4)

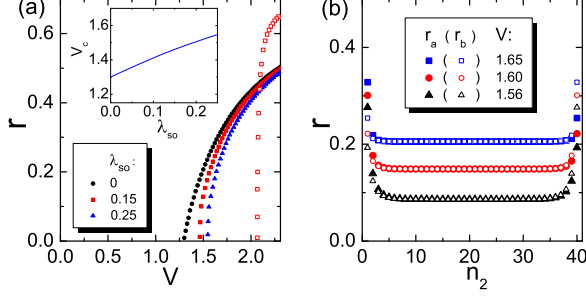


FIG. 3: (a) Large system with periodic boundary condition: The mean-field parameter r as a function of V for $\lambda_{so} = 0, 0.15$, and 0.25 . As a comparison, the red open square is for the corresponding single-ion Kondo problem for $\lambda_{so} = 0.15$. The inset shows the critical V_c as a function of λ_{so} . All the coupling constants are in unit of t . (b) The site-dependence of r for the lattice with zig-zag edges for several V in the Kondo phase, the width $N_2 = 40$, $\lambda_{so} = 0.15$.

giving rise to the quasiparticle dispersion

$$\begin{aligned} E_{\mathbf{k}}^{(1)} &= \frac{1}{2} \left(G_{\mathbf{k}+} + \sqrt{G_{\mathbf{k}-}^2 + 4r^2V^2} \right) - \mu \\ E_{\mathbf{k}}^{(2)} &= \frac{1}{2} \left(G_{\mathbf{k}-} + \sqrt{G_{\mathbf{k}+}^2 + 4r^2V^2} \right) - \mu \\ E_{\mathbf{k}}^{(3)} &= \frac{1}{2} \left(G_{\mathbf{k}+} - \sqrt{G_{\mathbf{k}-}^2 + 4r^2V^2} \right) - \mu \\ E_{\mathbf{k}}^{(4)} &= \frac{1}{2} \left(G_{\mathbf{k}-} - \sqrt{G_{\mathbf{k}+}^2 + 4r^2V^2} \right) - \mu \end{aligned} \quad (5)$$

with $G_{\mathbf{k}\pm} = E_0 + \lambda + \mu \pm \sqrt{\Lambda_{\mathbf{k}}^2 + |\epsilon_{\mathbf{k}}|^2}$. The parameters r and λ are determined by the following equations

$$\frac{1}{2N} \sum_{\mathbf{k}\sigma; \alpha=a,b} \langle f_{\alpha, \mathbf{k}\sigma}^\dagger f_{\alpha, \mathbf{k}\sigma} \rangle + r^2 = 1 \quad (6)$$

$$\frac{V}{2N} \sum_{\mathbf{k}\sigma; \alpha=a,b} \Re \langle c_{\alpha, \mathbf{k}\sigma}^\dagger f_{\alpha, \mathbf{k}\sigma} \rangle + r\lambda = 0 \quad (7)$$

with N being the total number of unit cells and \Re indicating the real part. In the following we shall mainly consider the half-filled case, corresponding to $\mu = 0$.

The formation of the quasiparticle bands, specified by Eq.(5), requires the renormalized hybridization $V^* = rV \neq 0$. By contrast, if $V^* = 0$, the spectra separate into the decoupled conduction bands and local level. Moreover, the band inversion takes place at $V^* = 0$. While this feature is hidden and not important in ordinary Kondo lattice problems, it is crucial in the present problem because now the conduction bands are from the TI. As a consequence, the bulk gap of TI closes at the onset of V^* , leading to a quantum phase transition to the KI.

At zero temperature, r (or V^*) is non-zero only if V is larger than a critical V_c , as a result of the suppressed density of conduction electron states for a honeycomb

lattice. Fig.3(a) shows the numerical results for the V -dependence of r for several values of λ_{so} . The local level E_0 is taken at the bottom of the conduction band. The critical $V_c \sim 1.3$ for $\lambda_{so} = 0$, and increases almost linearly with λ_{so} , as seen in the inset of Fig.3(a). When $V < V_c$, $r = 0$, indicating the Kondo destruction, so the system remains in the TI phase with a bulk gap $\Delta_T = 6\sqrt{3}\lambda_{so}$. While for $V > V_c$, $r \neq 0$, the Kondo screening emerges and the band inversion takes place immediately, so the system enters into the KI phase. For small r , the KI phase has a finite hybridization gap $\Delta_K \sim 2r^2V^2/3t$. This is the direct band gap at the Γ -point where the contribution from the SOC vanishes.

It is interesting to compare the results here for the Kondo-lattice problem with those for its counterpart of a single ion magnetic impurity imbedded in the bulk of the 2D TI. Using the same method, and for $\lambda_{so} = 0.15$ as an example shown in Fig.3(a), we find $V_c \sim 2.07$ for the single ion Kondo screening which is much larger than $V_c \sim 1.45$ determined here. In the absence of SOC, the finite V_c is due to the fact that the electron host is a pseudo gap system so that the single ion Kondo screening needs a nonzero Kondo coupling comparable to the gap amplitude³³⁻³⁵. The enhancement of Kondo effect comparing to the single ion Kondo screening is similar to the Kondo lattice with d -wave superconducting conduction electrons³⁶.

We next investigate the surface states of the finite system with boundaries. We take a 2D ribbon by cutting two zigzag edges with width N_2 , while the size along \mathbf{a}_1 remains infinite. Then the boson mean-field r is dependent on the coordinate n_2 and the sublattices, and can be denoted by $r_a(n_2)$ and $r_b(n_2)$ respectively. We have $r_b(n_2) = r_a(N_2 - n_2)$ due to the inversion symmetry. Fig.3(b) shows the site-dependence of r_a and r_b for $N_2 = 40$ and $\lambda_{so} = 0.15$. A general feature is that r decreases rapidly from the edge to the bulk. This feature is attributed to the gapless edge states. $r(n_2)$ is almost flat away from the edges ($5 < n_2 < 35$) as shown in Fig.3(b), indicating that the finite size effect is relatively small for $N_2 = 40$.

Figure 4 shows the energy spectra with four sets of parameters; here, $\mu = 0$ is imposed. Figs. 4(a) and (b) display the spectra of the conduction electrons in the absence of Kondo singlet ($V^* = 0$) and for $\lambda_{so} = 0, 0.03$, respectively. The edge states with a single Dirac point at the Fermi energy in Fig.4(b) manifest the TI phase^{9,25}. In comparison, Figs. 4 (c) and (d) are the spectra for $V > V_c$. The Kondo-singlet formation is clearly reflected in the hybridization gap at half-filling and the relatively narrow flat bands near the Fermi energy (near the transition point the flatness is measured by t/V^*).

Furthermore, we observe that in the KI phase, the narrow bands can be separated from the continuum by increasing the SOC, leading to a bulk gap at the 1/4- or 3/4- fillings (achieved by tuning the chemical potential $\mu \neq 0$). This is the direct band gap between $E_{\mathbf{k}}^{(3)}$ and $E_{\mathbf{k}}^{(4)}$ or between $E_{\mathbf{k}}^{(1)}$ and $E_{\mathbf{k}}^{(2)}$ at the points $(2\pi/3, 4\pi/3)$

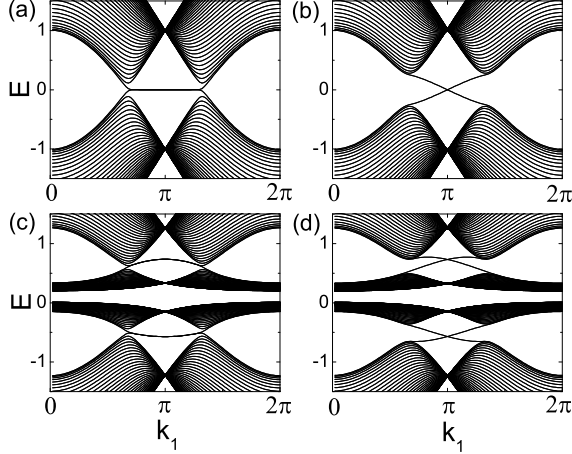


FIG. 4: The energy spectra for a ribbon of width $N_2 = 40$. (a) $V = 0$ and $\lambda_{so} = 0$; (b) $V = 0$ and $\lambda_{so} = 0.03$; (c) $V = 1.7$ and $\lambda_{so} = 0$; (d) $V = 1.7$ and $\lambda_{so} = 0.03$;

and $(4\pi/3, 2\pi/3)$, respectively, with the gap magnitude $\Delta_{KT} \sim 6\sqrt{3}r^2V^2\lambda_{so}/\mu^2$ for the large bulk system. Moreover, for the finite system with boundaries, the edge states emerge again with a Dirac point within the bulk gap. This feature is robust for a range of the chemical potential μ corresponding to the 1/4- or 3/4- filling. We have also calculated the \mathbb{Z}_2 topological bulk invariant Ξ_{2D} following the monodromy approach developed in Ref.³⁷. The result confirms that $\Xi_{2D} = 1$ at half-filling and $\Xi_{2D} = -1$ at 1/4- or 3/4-filling. Therefore, the insulating phase at 1/4- or 3/4-filling is topologically non-trivial, and its surface states, while having the spin direction locked by the momentum, contain the contributions from both conduction and local electrons. Hence in the case of Fig.4(d) we have a new TI phase with the Kondo-singlet formation and a surface heavy-fermion helical liquid.

We now consider the TI-KI transition around V_c . In the present analysis at the saddle-point level, the onset of Kondo effect is continuous (Fig. 3(a)). Correspondingly, the KI gap sets in continuously. By contrast, on the TI side there is simply a decoupling of the conduction-electron and local-moment components. However, we show that the quantum fluctuations beyond the saddle point reduce the bulk gap from the TI side, as is described in some detail in the Supplementary Materials (SM). The situation is similar to the case of single-impurity pseudo-gapped Kondo problem, for which numerical renormalization group calculations, for instance, establish a well-defined second-order phase transition for the Kondo-destruction quantum critical point³⁸. In the lattice case, the RKKY interaction between the local moments, which is mediated by Kondo coupling in our model, will also induce magnetic order. Taking into account the magnetic order will leave the KI phase intact;

as is standard, the Kondo screening present in the KI phase quenches the local moments and their ordering tendency. In the TI phase, we have explicitly shown (in the SM) that an antiferromagnetic order, characterized by the order parameter M , will reduce the TI bulk gap to $\Delta_T = 2(3\sqrt{3}\lambda_{so} - J_K M)(1 - \frac{(1-2I_R M)V^2}{2E_0^2})$. This TI gap remains non-zero for a finite range of M and V ; in other words, the TI phase remains stable in the presence of an antiferromagnetic order for a range of $V < V_c$. Our results can be understood based on general arguments: in the presence of magnetic order, the \mathbb{Z}_2 topological invariant is replaced by two spin-Chern numbers which remain unchanged when the time reversal symmetry is broken by the magnetic order^{5,6}. Meanwhile, the surface states remain gapless unless the bulk gap closes^{7,8}.

While a detailed transitions among KI and TI phases on the one hand, and antiferromagnetic order on the other is beyond the scope of the present work, our work does reveal that the heavy-fermion phase diagram contains a hitherto unexplored new regime with a competition among topological, Kondo-coherent and magnetic states; such competition involves the physics of Kondo destruction and associated local quantum criticality⁴³. In other words, when the magnetic order and related dynamical effects are incorporated in our analysis, the TI-KI transition discussed here will represent a regime where topological effects strongly interplay with the onset of magnetism and Kondo coherence. The simplification that proximity to quantum criticality brings may very well make the interaction effects on the TI phase and its associated surface states more tractable.

We close by noting that we have treated the hybridization to be \mathbf{k} -independent. When the spin- and \mathbf{k} -dependences of the hybridization is incorporated, part of the KI phase may itself become topological, as emphasized by Ref.²⁰.

We now briefly discuss our work in the context of 4f-electron-based Kondo insulators. In SmB_6 , it is known that a sufficiently large external pressure collapses the Kondo coherence in SmB_6 and turns it into an antiferromagnetic metallic state⁴⁴. Combined with the recent experimental evidence in SmB_6 for the edge states of a topological insulator^{23,24}, this is reminiscent of the transition among the topological and Kondo coherent/magnetic states implicated by the present study. An intriguing question then arises, which deserves the study of future experiments: what happens to the candidate chiral edge states when SmB_6 is placed under external pressure? Along a similar line, CeNiSn is another intermetallic system believed to be a Kondo insulator. In CeNiSn , (negative) chemical pressure achieved through Pd- or Pt- substitution for Ni is known to induce a transition out of its Kondo insulator state⁴⁵⁻⁴⁸. It will therefore be informative to explore surface states in the $\text{Ce}(\text{Pt}_{1-x}\text{Ni}_x)\text{Sn}$ and $\text{Ce}(\text{Pd}_{1-x}\text{Ni}_x)\text{Sn}$ series. Finally, it is worth noting that CePtSn has the distinction in that it involves 5d electrons with a large SOC.

To summarize, we have considered the effect of SOC

of the conduction electrons in a Kondo-lattice system. Our study offers the first qualitative understanding of the competition between topological and Kondo insulator ground states on a simple and yet generic model in two dimensions. While our analysis has so far been primarily confined to the paramagnetic cases, our results already suggest that the overall phase diagram of heavy-fermion systems includes a new regime with competition among topological, Kondo-coherent and magnetic states. This regime should be particularly prominent for heavy fermion systems whose conduction electron band is associated with the strongly spin-orbit-coupled $5d$ electrons. As such, our work opens up a new regime of physical

interest for compounds based on iridium, platinum and related $5d$ elements.

We would like to thank C. Cao, P. Goswami, E. Morosan, A. Nevidomskyy, and Y. Zhou for useful discussions. In particular, we thank S. Paschen for discussions on the Kondo-insulator materials. This work was supported in part by the NSF of China, the NSF of Zhejiang Province, the 973 Project of the MOST, the NSF Grant No.DMR-1006985, and the Robert A. Welch Foundation Grant No.C-1411. C.H.C. acknowledges support by the NSC Grant No.98-2918-I-009-06, No.98-2112-M-009-010-MY3, the NCTU-CTS, the NCTS, the MOE-ATU program of Taiwan.

-
- ¹ A.C. Hewson, *The Kondo Problem to Heavy Fermions*, Cambridge University Press, Cambridge, England, 1993.
 - ² P. Coleman, in *Handbook of Magnetism and Advanced Magnetic Materials*, V.1, 95 (Wiley, 2007).
 - ³ P. Gegenwart, Q. Si, and F. Steglich, *Nature Phys.* **4**, 186 (2008).
 - ⁴ G. Aeppli and Z. Fisk, *Comm. Condens. Matter Phys.* **16**, 155 (1992).
 - ⁵ H. Tsunetsugu, M. Sigrist, and K. Ueda, *Rev. Mod. Phys.* **69**, 809 (1997).
 - ⁶ P. Riseborough, *Adv. Phys.* **49**, 257 (2000).
 - ⁷ M.Z. Hasan and C.L. Kane, *Rev. Mod. Phys.* **82**, 3045 (2010).
 - ⁸ X.-L. Qi and S.-C. Zhang, *Rev. Mod. Phys.* **83**, 1057 (2011).
 - ⁹ C.L. Kane and E.J. Mele, *Phys. Rev. Lett.* **95**, 226801 (2005).
 - ¹⁰ C. Wu, B.A. Bernevig, and S.-C. Zhang, *Phys. Rev. Lett.* **96**, 106401 (2006).
 - ¹¹ J. Maciejko et al., *Phys. Rev. Lett.* **102**, 256803 (2009).
 - ¹² C.L. Kane and M.P.A. Fisher, *Phys. Rev. B* **46**, 15233 (1992).
 - ¹³ X.-Y. Feng et al., *Phys. Rev. B* **81**, 2345011 (2010).
 - ¹⁴ J. Gao, W. Chen, X.C. Xie, and F.-C. Zhang, *Phys. Rev. B* **80**, 241302 (2009).
 - ¹⁵ R.R. Biswas and A.V. Balatsky, *Phys. Rev. B* **81**, 233405 (2010).
 - ¹⁶ I. Garate and M. Franz, *Phys. Rev. Lett.* **104**, 146802 (2010).
 - ¹⁷ J.J. Zhu, D.X. Yao, S.C. Zhang, and K. Chang, *Phys. Rev. Lett.* **106**, 097201 (2011).
 - ¹⁸ See also, e.g., J. Maciejko, arXiv:1204.0017v1, unpublished, 2012.
 - ¹⁹ S. Nakatsuji et al., *Phys. Rev. Lett.* **96**, 087204 (2006).
 - ²⁰ M. Dzero, K. Sun, V. Galitski, and P. Coleman, *Phys. Rev. Lett.* **104**, 106408 (2010).
 - ²¹ M.X. Wang et al., *Science* **336**, 52 (2012).
 - ²² Y. Singh et al., *Phys. Rev. Lett.* **108**, 127203 (2012); Y. Singh and P. Gegenwart, *Phys. Rev. B* **82**, 064412 (2010).
 - ²³ S. Wolgast et al., arXiv:1211.5104, unpublished, 2012.
 - ²⁴ J. Botimer et al., arXiv:1211.6769, unpublished, 2012.
 - ²⁵ C.L. Kane and E.J. Mele, *Phys. Rev. Lett.* **95**, 146802 (2005).
 - ²⁶ S. Rachel and K. Le Hur, *Phys. Rev. B* **82**, 075106 (2010).
 - ²⁷ M. Hohenadler, T.C. Lang, and F.F. Assaad, *Phys. Rev. Lett.* **106**, 100403 (2011).
 - ²⁸ S.-L. Yu, X.C. Xie, and J.-X. Li, *Phys. Rev. Lett.* **107**, 010401 (2011).
 - ²⁹ D.-H. Lee, *Phys. Rev. Lett.* **107**, 166806 (2011).
 - ³⁰ D. Zheng, G.-M. Zhang, and C. Wu, *Phys. Rev. B* **84**, 205121 (2011).
 - ³¹ J. Quan et al., arXiv:1201.1698, unpublished, 2012.
 - ³² M. Dzero, arXiv:1204.1886, unpublished, 2012.
 - ³³ D. Withoff and E. Fradkin, *Phys. Rev. Lett.* **64**, 1835 (1990).
 - ³⁴ K. Ingersent, *Phys. Rev. B* **54**, 11936 (1996).
 - ³⁵ B. Uchoa, T.G. Rappoport, and A.H. Castro Neto, *Phys. Rev. Lett.* **106**, 016801 (2011).
 - ³⁶ D.E. Sheehy and J. Schmalian, *Phys. Rev. B* **77**, 125129 (2008).
 - ³⁷ E. Prodan, *Phys. Rev. B* **83**, 235115 (2011).
 - ³⁸ K. Ingersent and Q. Si, *Phys. Rev. Lett.* **89**, 076403 (2002).
 - ³⁹ D.N. Sheng, Z.Y. Weng, L. Sheng, and F.D.M. Haldane, *Phys. Rev. Lett.* **97**, 036808 (2006).
 - ⁴⁰ E. Prodan, *Phys. Rev. B* **80**, 125327 (2009).
 - ⁴¹ Y. Yang et al., *Phys. Rev. Lett.* **107**, 066602 (2011).
 - ⁴² H. Li, L. Sheng, and D.Y. Xing, *Phys. Rev. Lett.* **108**, 196806 (2012).
 - ⁴³ S. J. Yamamoto and Q. Si, *J. Low Temp. Phys.* **161**, 233 (2010).
 - ⁴⁴ A. Barla, J. Derr, J.P. Sanchez, B. Salce, G. Lapertot, B.P. Doyle, R. Rüffer, R. Lengsdorf, M.M. Abd-Elmeguid, and J. Flouquet, *Phys. Rev. Lett.* **94**, 166401 (2005).
 - ⁴⁵ J. Sakurai, R. Kawamura, T. Taniguchi, S. Nishigori, S. Ikeda, H. Goshima, T. Suzuki, and T. Fujita, *J. Magn. Mater.* **104-107**, 1415 (1992).
 - ⁴⁶ D.T. Adroja, B.D. Rainford, A.J. Neville, and A.G.M. Jansen, *Physica B* **223&224**, 275 (1996).
 - ⁴⁷ G.M. Kalvius, A. Kratzer, G. Grosse, D.R. Noakes, R. Wäppling, H. v. Löhneysen, T. Takabatake, and Y. Echizen, *Physica B* **289&290**, 256 (2000).
 - ⁴⁸ M. Kasaya, T. Tani, H. Suzuki, K. Ohoyama, and M. Kohgi, *J. Phys. Soc. Jpn.* **60**, 2542 (1991).
-

Supplementary Material – Competing topological and Kondo insulator phases on a honeycomb lattice

by: Xiao-Yong Feng, Jianhui Dai, Chung-Hou Chung, Qimiao Si

In this Supplementary Material, we first derive an effective action of the Kondo lattice model with SOC by taking into account the quantum fluctuations of the slave bosons. We show that while the quantum fluctuations do not affect the Kondo insulator (KI) phase, they do reduce the bulk gap of the topological insulator (TI) phase. We then consider the effect of the magnetic order of the local spins, which breaks the time-reversal symmetry. We show that the magnetic order does not change the nature of the TI phase. The notations here follow those introduced in the main text.

A. Effect of quantum fluctuations beyond the saddle point

We start from expressing the Hamiltonian introduced in the main text in the slave-boson representation,

$$H = -t \sum_{\langle ij \rangle \alpha} c_{i\sigma}^\dagger c_{j\sigma} + i\lambda_{so} \sum_{\ll ij \gg \sigma\sigma'} v_{ij} c_{i\sigma}^\dagger s_{\sigma\sigma'}^z c_{j\sigma'} - \mu \sum_{i\alpha} c_{i\sigma}^\dagger c_{i\sigma} \quad (S1)$$

$$+ V \sum_{i\sigma} (c_{i\sigma}^\dagger b_i^\dagger f_{i\sigma} + f_{i\sigma}^\dagger b_i c_{i\sigma}) + (E_0 + \lambda) \sum_{i\sigma} f_{i\sigma}^\dagger f_{i\sigma} + \lambda \sum_i b_i^\dagger b_i \quad (S2)$$

$$= \sum_{\mathbf{k}\sigma} (c_{a,\mathbf{k}\sigma}^\dagger, c_{b,\mathbf{k}\sigma}^\dagger) \begin{pmatrix} -\mu + \sigma\Lambda_{\mathbf{k}} & \epsilon_{\mathbf{k}} \\ \epsilon_{\mathbf{k}}^* & -\mu - \sigma\Lambda_{\mathbf{k}} \end{pmatrix} \begin{pmatrix} c_{a,\mathbf{k}\sigma} \\ c_{b,\mathbf{k}\sigma} \end{pmatrix} \quad (S3)$$

$$+ \frac{V}{\sqrt{N}} \sum_{\alpha\mathbf{k}\mathbf{q}\sigma} (c_{\alpha,\mathbf{k}-\mathbf{q}\sigma}^\dagger b_{\alpha,\mathbf{q}}^\dagger f_{\alpha,\mathbf{k}\sigma} + f_{\alpha,\mathbf{k}\sigma}^\dagger b_{\alpha,\mathbf{q}} c_{\alpha,\mathbf{k}-\mathbf{q}\sigma}) + (E_0 + \lambda) \sum_{\alpha\mathbf{k}\sigma} f_{\alpha,\mathbf{k}\sigma}^\dagger f_{\alpha,\mathbf{k}\sigma} + \lambda \sum_{\alpha\mathbf{q}} b_{\alpha,\mathbf{q}}^\dagger b_{\alpha,\mathbf{q}} \quad (S4)$$

In the above expression, $\alpha = a$ or b is the index for sublattices, λ is introduced to implement the no double occupation of local electrons. In this formulism, the bosons can accommodate zero modes, which are denoted by $b_{\alpha,\mathbf{q}=0}^\dagger = b_{\alpha,\mathbf{q}=0} = r\sqrt{N}$. Hence a nonvanishing r corresponds to the Bose-Einstein condensation of the slave-bosons. Quantum fluctuations are contributed mainly from the bosons with non-zero \mathbf{q} . The effective action S_{eff} for the system, defined by $Tr e^{-\beta H} = \int \mathcal{D}c_{\alpha,\mathbf{k}\sigma}^* \mathcal{D}c_{\alpha,\mathbf{k}\sigma} \mathcal{D}f_{\alpha,\mathbf{k}\sigma}^* \mathcal{D}f_{\alpha,\mathbf{k}\sigma} \mathcal{D}b_{\alpha,\mathbf{q}}^* \mathcal{D}b_{\alpha,\mathbf{q}} e^{-S_{eff}}$, is then given by

$$S_{eff} = S_c + \sum_{\alpha\mathbf{k}\omega\sigma} f_{\alpha,\mathbf{k}\sigma}^*(\omega)(-i\omega + E_0 + \lambda)f_{\alpha,\mathbf{k}\sigma}(\omega) + \sum_{\alpha\mathbf{q}\neq 0,\Omega} b_{\alpha,\mathbf{q}}^*(-i\Omega + \lambda)b_{\alpha,\mathbf{q}} \quad (S5)$$

$$+ \left[V \sum_{\alpha\mathbf{k}\omega\sigma} \left(r c_{\alpha,\mathbf{k}\sigma}^*(\omega) + \frac{1}{\sqrt{N\beta}} \sum_{\mathbf{q}\neq 0,\Omega} c_{\alpha,\mathbf{k}-\mathbf{q}\sigma}^*(\omega - \Omega) b_{\alpha,\mathbf{q}}^*(\Omega) \right) f_{\alpha,\mathbf{k}\sigma}(\omega) + c.c \right]. \quad (S6)$$

Here,

$$S_c = \sum_{\mathbf{k}\omega\sigma} (c_{a,\mathbf{k}\sigma}^*(\omega), c_{b,\mathbf{k}\sigma}^*(\omega)) \begin{pmatrix} -i\omega - \mu + \sigma\Lambda_{\mathbf{k}} & \epsilon_{\mathbf{k}} \\ \epsilon_{\mathbf{k}}^* & -i\omega - \mu - \sigma\Lambda_{\mathbf{k}} \end{pmatrix} \begin{pmatrix} c_{a,\mathbf{k}\sigma}(\omega) \\ c_{b,\mathbf{k}\sigma}(\omega) \end{pmatrix} \quad (S7)$$

is the bare action of the itinerant electrons, $\omega = \frac{(2n+1)\pi}{\beta}$ ($\Omega = \frac{2n\pi}{\beta}$) are the Matsubara frequencies for fermions (bosons). After integrating out the fermionic (Grassman) fields $f_{\alpha,\mathbf{k}\sigma}(\omega)$ and $f_{\alpha,\mathbf{k}\sigma}^*(\omega)$, the effective action becomes

$$S = S_c + \sum_{\alpha\mathbf{q}\neq 0,\Omega} b_{\alpha,\mathbf{q}}^*(-i\Omega + \lambda)b_{\alpha,\mathbf{q}} - \sum_{\alpha\mathbf{k}\omega\sigma} \frac{V^2 r^2}{-i\omega + E_0 + \lambda} c_{\alpha,\mathbf{k}\sigma}^*(\omega) c_{\alpha,\mathbf{k}\sigma}(\omega) \quad (S8)$$

$$- \frac{1}{N\beta} \sum_{\alpha\mathbf{k}\omega\mathbf{q}\neq 0,\mathbf{q}'\neq 0,\Omega,\Omega',\sigma} \frac{V^2}{-i\omega + E_0 + \lambda} c_{\alpha,\mathbf{k}-\mathbf{q}\sigma}^*(\omega - \Omega) c_{\alpha,\mathbf{k}-\mathbf{q}'\sigma}(\omega - \Omega') b_{\alpha,\mathbf{q}}^*(\Omega) b_{\alpha,\mathbf{q}'}(\Omega'). \quad (S9)$$

We integrate out the bosonic fields and, to order of V^2 , obtain the following effective action for the conduction electrons

$$S_{eff} = S_c - \sum_{\alpha \mathbf{k} \omega \sigma} \frac{V^2 r^2}{-i\omega + E_0 + \lambda} c_{\alpha, \mathbf{k}\sigma}^*(\omega) c_{\alpha, \mathbf{k}\sigma}(\omega) \quad (\text{S10})$$

$$- \frac{1}{\beta} \sum_{\alpha \mathbf{k} \omega \Omega \sigma} \frac{V^2}{(i\Omega - \lambda)[i(\omega - \Omega) - E_0 - \lambda]} c_{\alpha, \mathbf{k}\sigma}^*(\omega) c_{\alpha, \mathbf{k}\sigma}(\omega) + \mathcal{O}(V^4). \quad (\text{S11})$$

Now using the identities,

$$\frac{1}{(i\Omega - \lambda)[i(\omega + \Omega) - E_0 - \lambda]} = \frac{1}{i\omega - E_0} \left(\frac{1}{i\Omega - \lambda} - \frac{1}{i(\omega + \Omega) - E_0 - \lambda} \right), \quad (\text{S12})$$

$$\frac{1}{\beta} \sum_{\Omega} \frac{1}{i\Omega - \lambda} = -n_B(\lambda) = 0, \quad (\text{S13})$$

$$\frac{1}{\beta} \sum_{\Omega} \frac{1}{i(\omega + \Omega) - E_0 - \lambda} = n_F(E_0 + \lambda), \quad (\text{S14})$$

we arrive at the following expression for the effective action

$$S_{eff} = \sum_{\mathbf{k} \omega \sigma} (c_{a, \mathbf{k}\sigma}^*(\omega), c_{b, \mathbf{k}\sigma}^*(\omega)) G_{\sigma}(\mathbf{k}, \omega)^{-1} \begin{pmatrix} c_{a, \mathbf{k}\sigma}(\omega) \\ c_{b, \mathbf{k}\sigma}(\omega) \end{pmatrix}, \quad (\text{S15})$$

where the inverse of the Green's function is

$$G_{\sigma}(\mathbf{k}, \omega)^{-1} = \begin{pmatrix} -i\omega + \frac{n_F(E_0 + \lambda)V^2}{i\omega - E_0} + \frac{V^2 r^2}{i\omega - E_0 - \lambda} - \mu + \sigma \Lambda_{\mathbf{k}} & \epsilon_{\mathbf{k}} \\ \epsilon_{\mathbf{k}}^* & -i\omega + \frac{n_F(E_0 + \lambda)V^2}{i\omega - E_0} + \frac{V^2 r^2}{i\omega - E_0 - \lambda} - \mu - \sigma \Lambda_{\mathbf{k}} \end{pmatrix}. \quad (\text{S16})$$

Since the bare energy level of the local f -electrons $E_0 < 0$ is much lower than the Fermi energy, the poles of the Green's function are essentially determined by the condition $E_0 + \lambda \sim 0$ when $r \neq 0$. In this case, one recovers all the mean-field results as discussed in the main text, where the quasiparticle bands are equivalently given by the poles of the Green's function. The Kondo regime where $r \neq 0$ is determined by $V > V_c$, with V_c being self-consistently solved by the mean field equations. Quantum fluctuations contributed from the term $\frac{n_F(E_0 + \lambda)V^2}{i\omega - E_0}$ are negligible. Therefore we conclude that the existence of the KI phase and its properties are robust to the quantum fluctuations of the slave bosons.

On the other hand, when $V < V_c$, or $r = 0$, one has $n_F(E_0 + \lambda) = \frac{1}{2}$, then the poles of the Green's function are given by

$$\omega_1 = \frac{1}{2} \left[-(\mu + \sqrt{\Lambda_{\mathbf{k}}^2 + |\epsilon_{\mathbf{k}}|^2} - E_0) + \sqrt{(\mu + \sqrt{\Lambda_{\mathbf{k}}^2 + |\epsilon_{\mathbf{k}}|^2} + E_0)^2 + 2V^2} \right] \quad (\text{S17})$$

$$\omega_2 = \frac{1}{2} \left[-(\mu - \sqrt{\Lambda_{\mathbf{k}}^2 + |\epsilon_{\mathbf{k}}|^2} - E_0) + \sqrt{(\mu - \sqrt{\Lambda_{\mathbf{k}}^2 + |\epsilon_{\mathbf{k}}|^2} + E_0)^2 + 2V^2} \right] \quad (\text{S18})$$

$$\omega_3 = \frac{1}{2} \left[-(\mu + \sqrt{\Lambda_{\mathbf{k}}^2 + |\epsilon_{\mathbf{k}}|^2} - E_0) - \sqrt{(\mu + \sqrt{\Lambda_{\mathbf{k}}^2 + |\epsilon_{\mathbf{k}}|^2} + E_0)^2 + 2V^2} \right] \quad (\text{S19})$$

$$\omega_4 = \frac{1}{2} \left[-(\mu - \sqrt{\Lambda_{\mathbf{k}}^2 + |\epsilon_{\mathbf{k}}|^2} - E_0) - \sqrt{(\mu - \sqrt{\Lambda_{\mathbf{k}}^2 + |\epsilon_{\mathbf{k}}|^2} + E_0)^2 + 2V^2} \right] \quad (\text{S20})$$

At the half filling, $\mu = 0$, there are two quasiparticle bands near the Fermi energy, ω_1 and ω_2 . While the bands ω_3 and ω_4 are well below the Fermi energy and are always occupied. When $V = 0$, one simply recovers the two electron bands decoupled from the local spins, with a direct band gap between ω_1 and ω_2 opens at the Dirac points, $\frac{1}{2}\Delta_T = \sqrt{\Lambda_{\mathbf{k}}^2 + |\epsilon_{\mathbf{k}}|^2} = 3\sqrt{3}\lambda_{so}$. When $V(< V_c)$ is small, the band structures do not change, while the amplitude of the band gap is given by $\Delta_T(1 - \frac{V^2}{2E_0^2})$. Therefore, the hybridization $V(< V_c)$ just reduces the bulk gap of the TI phase. Combined with the result shown in Fig.3(a), our results suggest that the bulk gap decreases continuously when the quantum critical point is approached from either sides. Therefore we argue that quantum fluctuations turn the TI-KI transition into a canonical continuous form, with vanishing gaps from both sides.

B. Effect of antiferromagnetic order of the local spins

We turn consider an antiferromagnetic order of the local spins induced by the RKKY interactions. Our main concern here is how such an order, which breaks the time-reversal symmetry, influences the topological order. To address this issue, it is adequate to consider the effect of an effective staggered magnetic field associated with the antiferromagnetic order. For definiteness, we consider the antiferromagnetic order to correspond to the local spins staggered on the sublattices a and b. We use M to represent the magnetization of the f -electrons per site in the even (or odd) sublattice, which will induce a conduction-electron polarization by the Kondo interaction. This will add an additional term The effective Hamiltonian is:

$$H_J = \sum_{a\mathbf{k}\sigma} \sigma I_R M f_{a,\mathbf{k}\sigma}^\dagger f_{a,\mathbf{k}\sigma} - \sum_{b\mathbf{k}\sigma} \sigma I_R M f_{b,\mathbf{k}\sigma}^\dagger f_{b,\mathbf{k}\sigma} - \sum_{a\mathbf{k}\sigma} \sigma J_K M c_{a,\mathbf{k}\sigma}^\dagger c_{a,\mathbf{k}\sigma} + \sum_{b\mathbf{k}\sigma} \sigma J_K M c_{b,\mathbf{k}\sigma}^\dagger c_{b,\mathbf{k}\sigma} \quad (\text{S21})$$

to the total Hamiltonian. Here, I_R is the RKKY interaction $\sim \rho_0 J_K^2$, which is small for small hybridization.

We follow the approach similar to what was described above, obtaining the inverse Green's function in the TI phase ($V < V_c$)

$$G_\sigma(\mathbf{k}, \omega)^{-1} = \begin{pmatrix} -i\omega + \frac{n_F(E_0 + \lambda + \sigma I_R M) V^2}{i\omega - E_0 - \sigma I_R M} - \mu + \sigma(\Lambda_{\mathbf{k}} - J_K M) & \epsilon_{\mathbf{k}} \\ \epsilon_{\mathbf{k}}^* & -i\omega + \frac{n_F(E_0 + \lambda - \sigma I_R M) V^2}{i\omega - E_0 + \sigma I_R M} - \mu - \sigma(\Lambda_{\mathbf{k}} - J_K M) \end{pmatrix} \quad (\text{S22})$$

Because in the absence of $I_R M$, $(E_0 + \lambda)$ is close to 0 at half-filling, it is reasonable to replace $n_F(E_0 + \lambda + \sigma I_R M)$ by $1/2 - \sigma I_R M$ when M is very small. Then, with the first order approximation, $\frac{n_F(E_0 + \lambda + \sigma I_R M) V^2}{i\omega - E_0 - \sigma I_R M} \sim \frac{V^2}{2(i\omega - E_0)} - \sigma \frac{I_R M V^2}{i\omega - E_0}$. Therefore, the poles of the Green's function is given by

$$[-\omega + \frac{V^2}{2(\omega - E_0)} - \frac{I_R M V^2}{\omega - E_0} + (\Lambda_{\mathbf{k}} - J_K M)][-\omega + \frac{V^2}{2(\omega - E_0)} + \frac{I_R M V^2}{\omega - E_0} - (\Lambda_{\mathbf{k}} - J_K M)] = |\epsilon_{\mathbf{k}}|^2.$$

Obviously, the quasiparticle bands are similar to those of the original TI phase. At the gap position, $\epsilon_{\mathbf{k}} = 0$, $\omega - \frac{V^2(1 \mp 2I_R M)}{2(\omega - E_0)} = \pm(\Lambda_{\mathbf{k}} - J_K M)$. The effect of the staggered fields (M) is evident: while M simply reduces the energy $\Lambda_{\mathbf{k}}$, it also effectively renormalizes $V^2 \rightarrow V^2(1 \mp 2I_R M)$. They both reduce the direct bulk gap as $2(3\sqrt{3}\lambda_{so} - J_K M)[1 - \frac{V^2(1+2M)}{2E_0^2}]$ at the Dirac points. Because the magnetic order breaks the time reversal symmetry (TRS), the spin degeneracy of the surface states splits¹. It is well-known that the TI with a TRS-breaking magnetic field is characterized by the spin Chern number²⁻⁴, and the Z_2 characterization is recovered continuously when $M \rightarrow 0$ ^{5,6}. Hence the TI phase persists when $M \neq 0$ unless the bulk gap Δ closes at certain large and finite hybridization ($I_R M$ and $J_K M$). Therefore, we conclude that for small hybridization, the antiferromagnetic order keeps the KI phase intact. This demonstrates the validity of the main conclusions obtained from the SBMF method. For sufficient large hybridization ($I_R M$ and $J_K M$), however, the system enters the antiferromagnetic phase in which the surface states may be gapped^{7,8}. The band structures at that regime are rich but beyond the scope of the present paper.

¹ C.L. Kane and E.J. Mele, Phys. Rev. Lett. **95**, 146802 (2005).

² F.D.M. Haldane, Phys. Rev. Lett. **61**, 2015 (1988).

³ X.L. Qi, Y.S. Wu, and S.C. Zhang, Phys. Rev. B **74**, 045125 (2006).

⁴ T. Fukui and Y. Hatsugai, Phys. Rev. B **75**, 121403(R) (2007).

⁵ D.N. Sheng, Z.Y. Weng, L. Sheng, and F.D.M. Haldane, Phys. Rev. Lett. **97**, 036808 (2006).

⁶ E. Prodan, Phys. Rev. B **80**, 125327 (2009).

⁷ Y. Yang et al., Phys. Rev. Lett. **107**, 066602 (2011).

⁸ H. Li, L. Sheng, and D.Y. Xing, Phys. Rev. Lett. **108**, 196806 (2012).